

Magnetoelastic coupling in BaTiO₃-based multiferroic structures

C. A. F. Vaz*

*Department of Applied Physics, Yale University, New Haven, Connecticut 06520 and
Center for Research on Interface Structures and Phenomena (CRISP),
Yale University, New Haven, Connecticut 06520*

(Dated: November 2, 2018)

Analytical expressions for the magnetoelastic anisotropy constants of cubic magnetic systems are derived for rectangular and oblique distortions originating from epitaxial growth on substrates with lower crystal symmetry. In particular, the temperature variation of the magnetic properties of magnetic films grown on barium titanate (BaTiO₃) substrates are explained in terms of strain-induced magnetic anisotropies caused by the temperature dependent phase transitions of BaTiO₃. Our results quantify the experimental observations in ferromagnet/BaTiO₃-based structures, which have been proposed as templates for magnetoelectric composite heterostructures.

PACS numbers: 75.30.Gw, 75.70.-i, 77.84.-s, 75.80.+q

I. INTRODUCTION

Complex oxides are characterized by a strong coupling between charge, spin and lattice distortions, giving rise to a rich variety of electronic and magnetic behavior which is at the origin of the multifunctional properties exhibited by this class of materials. In particular, much effort is being made towards the control of these properties by means of electric and magnetic fields. While intrinsic multiferroic materials already exhibit a coupling between magnetic and electric order parameters,^{1,2,3,4} the magnitude of the coupling in these compounds is weak, and a new class of composite materials is being developed that exploit the different properties of the constituent compounds to tailor systems with larger susceptibilities and more varied response functions than those of single component systems.

In this context, the cross coupling in ferroelectric/magnetic heterostructures and composite materials is being intensively studied. The coupling mechanism can be classified as strain-driven or charge driven: in the first case, the piezoelectric effect of ferroelectrics is used to modify the magnetic properties of ferro- or ferrimagnets via magnetoelastic coupling;^{4,5,6,7,8} in the second case, the coupling originates from modifications in the electronic properties of the magnetic system driven by charge modulation induced by the polarization state of the ferroelectric.⁹

A particular case of strain-mediated magnetoelectric coupling occurs in epitaxial heterostructures composed of thin magnetic films grown on BaTiO₃ single crystals, including La_{1-x}Sr_xMnO₃,^{10,11,12} SrRuO₃,¹¹ CoFe₂O₄,¹³ Fe,¹⁴ and Fe₃O₄,^{15,16,17} where the changes in strain occur as a function of temperature via the phase transitions of BaTiO₃ or via applied electric fields. However, to date, the magnetoelastic coupling has not been addressed explicitly in detail. Here, we present analytical

expressions for the magnetoelastic contributions to the magnetic anisotropy induced by elastic coupling between the different phases of the BaTiO₃ substrate to the epitaxial magnetic film. This coupling explains the magnetic behavior exhibited by these systems as a function of temperature in terms of the changes in the magnetoelastic anisotropies.

BaTiO₃ has a simple perovskite structure at high temperatures and undergoes several crystal phase transitions as a function of temperature.^{18,19} It is cubic in the temperature range from ~ 1733 K to ~ 393 K ($a = 3.996$ Å at 393 K), tetragonal at temperatures down to ~ 278 K ($a = 3.9920$ Å and $c = 4.0361$ Å at 293 K), orthorhombic down to ~ 183 K ($a_o = 5.669$ Å, $b_o = 5.682$ Å, and $c_o = 3.990$ Å at $T = 263$ K), and rhombohedral at lower temperatures ($a = 4.001$ Å, $\gamma = 89.85^\circ$ at 105 K). For temperatures below ~ 393 K, BaTiO₃ is ferroelectric. The non-cubic lattices correspond to slight distortions of the cubic phase, with the direction of the distortion linked to that of the electric polarization, \mathbf{P} .^{18,19} In the tetragonal phase the electric polarization points along the c axis; in the orthorhombic phase, the spontaneous polarization points along the $\langle 110 \rangle$ directions of the cubic cell, leading to a slight elongation of the unit cell along that direction. Although the symmetry group is orthorhombic, with lattice parameters a_o , b_o , and c_o when \mathbf{P} points along $[110]$, it is often convenient to consider the monoclinic cell with $a_m = b_m = (a_o^2 + b_o^2)^{1/2}/2$ and $\gamma = 2 \arctan(a_o/b_o)$, giving $a = b = 4.013$ Å, $c = 3.99$ Å, $\gamma = 89.869^\circ$ at $T = 263$ K. For the rhombohedral phase, the polarization points along the $\langle 111 \rangle$ directions of the cubic cell, corresponding to an elongation of the cubic cell along \mathbf{P} .

II. MAGNETO-ELASTIC ENERGY EXPRESSIONS

In the following, we are interested in determining the effect of the in-plane strain on the anisotropy constants of ferromagnetic (or ferrimagnetic) films due to magne-

*Email: carlos.vaz@yale.edu

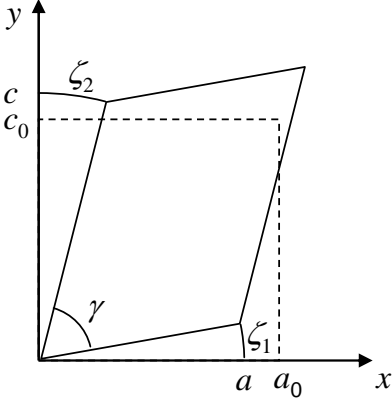


FIG. 1: Schematic of a general (oblique) distortion of a rectangular unit cell. The strain components correspond to the normalized difference between the distorted and the original equilibrium unit cell.

toelastic coupling. We assume that the strain propagates uniformly throughout the film. When relaxation occurs, as is often the case in real systems, the expressions below correspond to upper bounds to the magnetoelastic anisotropy induced in the magnetic system. If the residual strain is known, the effective anisotropies can be estimated.

To calculate the magnetoelastic anisotropy contributions arising from strain, we minimize the sum of the elastic (F_{elas}) and magnetoelastic (F_{me}) energies for a given strain state of the system. We consider the case of a cubic magnetic system:^{20,21,22}

$$F_{\text{me}} = b_1 \sum_i \alpha_i^2 \epsilon_{ii} + b_2 \sum_{i>j} \alpha_i \alpha_j \epsilon_{ij} \quad (1)$$

$$F_{\text{elas}} = \frac{c_{11}}{2} \sum_i \epsilon_{ii}^2 + c_{12} \sum_{i>j} \epsilon_{ii} \epsilon_{jj} + \frac{c_{44}}{2} \sum_{i>j} \epsilon_{ij}^2, \quad (2)$$

where α_i are the direction cosines of the magnetization, ϵ_{ij} are the components of the strain tensor, b_i are the magnetoelastic coupling coefficients, c_{ij} are the elastic constants and i, j are the cartesian coordinate indexes. The magnetoelastic constants are related to the magnetostriction coefficients by:²⁰

$$b_1 = -3(c_{11} - c_{12})\lambda_{100}/2 \quad (3)$$

$$b_2 = -3c_{44}\lambda_{111} \quad (4)$$

For a general in-plane distortion in a cubic lattice, it is straightforward to calculate the in-plane strain tensor components, since by definition the latter correspond to the relative deviations from the equilibrium lattice constant; with the aid of Fig. 1, we find:

$$\epsilon_{xx} = (a \cos \zeta_1 - a_0)/a_0 \quad (5)$$

$$\epsilon_{yy} = (c \cos \zeta_2 - c_0)/c_0 \quad (6)$$

$$\epsilon_{xy} = [(a/a_0) \sin \zeta_1 + (c/c_0) \sin \zeta_2]/2, \quad (7)$$

where a_0, c_0 are the equilibrium in-plane lattice parameters of the magnetic film and a, c, γ and ζ are the

parameters characterizing the planar lattice distortion. Here, we discuss the case of a (001) ferromagnetic film, where $a_0 = c_0$, but the calculations can be easily modified for other cases. The out of plane strain components are free to settle to the values that minimize the total energy (zero out of plane stress). The magnetoelastic anisotropy is then calculated by finding the minimum of $F_m = F_{\text{me}} + F_{\text{elas}}$ with respect to $\epsilon_{xz}, \epsilon_{yz}$ and ϵ_{zz} :

$$\epsilon_{zz} = -\frac{c_{12}}{c_{11}}(\epsilon_{xx} + \epsilon_{yy}) - \frac{b_1}{c_{11}}\alpha_z^2 \quad (8)$$

$$\epsilon_{xz} = -\frac{b_2}{c_{44}}\alpha_x \alpha_z \quad (9)$$

$$\epsilon_{yz} = -\frac{b_2}{c_{44}}\alpha_y \alpha_z; \quad (10)$$

inserting (8-10) into the expression for F_m gives, retaining only the terms that depend on the magnetization:

$$F_m = b_1 \left[\epsilon_{xx} \alpha_x^2 + \epsilon_{yy} \alpha_y^2 - \frac{c_{12}}{c_{11}}(\epsilon_{xx} + \epsilon_{yy}) \alpha_z^2 \right] + b_2 \epsilon_{xy} \alpha_x \alpha_y + o(b^2/c) \quad (11)$$

where the last term is strain independent, corresponding to a sum of terms of the order of b_1^2/c_{11} and b_2^2/c_{44} with α_z^2 and α_z^4 dependencies. These are much smaller than the first terms and will be ignored in the following discussion. They arise from a shear strain exerted by the magnetization on the lattice (which favors specific directions that depend on the relative sign of the magnetoelastic coupling coefficients) and are usually neglected to first order of approximation. We note that the magnetoelastic terms are uniaxial and lower in symmetry than the magnetocrystalline anisotropy of the unstrained cubic magnetic system.

A more convenient expression is obtained by using spherical coordinates, where the polar axis is set along the out of plane direction:

$$F_m = \frac{1}{2} [b_1(\epsilon_{xx} - \epsilon_{yy}) \cos 2\phi + b_2 \epsilon_{xy} \sin 2\phi] \sin^2 \theta - \frac{b_1}{2} (1 + 2c_{12}/c_{11})(\epsilon_{xx} + \epsilon_{yy}) \cos^2 \theta \quad (12)$$

where the first two terms correspond to in-plane magnetoelastic anisotropies, and the last term is the perpendicular magnetoelastic anisotropy contribution. An in-plane uniaxial anisotropy arises for uniaxial in-plane strains ($\epsilon_{xx} \neq \epsilon_{yy}$) or for shear strains, although the anisotropy direction is distinct for these two cases: in the first case, it is oriented along the main crystal axes, while for shear strains, the anisotropy is directed along the in-plane diagonal directions. A perpendicular anisotropy arises when $\epsilon_{zz} \neq 0$. The relative magnitude of $b_1 \epsilon_{zz}$ with respect to the magnetostatic energy term (shape anisotropy, which favors in-plane magnetization), which is on the order of $2\pi M_s^2$, where M_s is the saturation magnetization, determines whether a state of in-plane or perpendicular magnetization is favored. For the particular case of a

biaxial strain ($\epsilon_{xx} = \epsilon_{yy}$, $\epsilon_{xy} = 0$), the magnetoelastic anisotropy energy reduces to a perpendicular magnetic anisotropy term only, with $K_p = -b_1(1 + 2c_{12}/c_{11})\epsilon_{xx}$, as expected.²³

We consider next the effect of square, rectangular, oblique and rhomboidal distortions on the magnetoelastic anisotropy. These planar domains arise in the cubic, tetragonal, orthorhombic and rhombohedral phases of BaTiO₃, and are responsible for the large magnetic anisotropy modulations observed in ferromagnetic/BaTiO₃(001) heterostructures. We consider the magnetoelastic anisotropy constants, K_t , K_o , K_p , expressed as:

$$F_m = [K_t \cos 2\phi + K_o \sin 2\phi] \sin^2 \theta + K_p \cos^2 \theta. \quad (13)$$

The direction of easy magnetization depends on the particular K values; positive K_p favors in-plane magnetization. The magnetoelastic anisotropy for the cubic phase of BaTiO₃ ($\zeta_1 = \zeta_2 = 0$, $a = c$) leads to zero in-plane anisotropy. For the tetragonal phase ($\zeta_1 = \zeta_2 = 0$), two types of domains are possible, c -domains (square) and a -domains (rectangular, which may co-exist in two orthogonal directions). A multidomain state can arise when cooling the BaTiO₃ from the cubic to the tetragonal phase after film growth at elevated temperatures, for example. For this phase, no shear strains are present and $K_o = 0$. The orthorhombic phase may give rise to (two) rectangular ($\zeta_1 = \zeta_2 = 0$, $a \neq c$) and (two) oblique ($\zeta_1 = \zeta_2$, $a = c$) domains. Finally, the rhombohedral phase ($\zeta_1 = \zeta_2$, $a = c$) is characterized by (two) oblique domains. It also follows that for the oblique domains of the orthorhombic and rhombohedral phases of BaTiO₃, $K_t = 0$.

III. APPLICATION TO EPITAXIAL MAGNETIC FILMS

In general, it may be difficult to control the ferroelectric state of BaTiO₃ across the different phase transitions. For example, the growth of oxide magnetic films is often carried out at elevated temperatures, where BaTiO₃ is cubic and, as the temperature is lowered to room temperature, the BaTiO₃ tends to break into a ferroelectric multidomain state, giving rise to a and c domains in a BaTiO₃(001) single crystal. Similar processes operate at the other phase transitions, leading to the presence of different types of planar domains at the interface with the magnetic film. In such cases, an effective magnetoelastic anisotropy corresponds to an average over the relative number and size of domains present; in the case where an equal number of the two possible oblique domains are present in the rhombohedral phase, no effective in-plane anisotropy would result. However, experimental estimates of the relative population of the different domains is difficult. In the following we will consider single domain states; for similar, but orthogonal, domains, the in-plane anisotropy constants will be

identical, but with opposite signs, while the perpendicular anisotropies are unaffected. Another difficulty relates to the fact that for systems with large lattice mismatch, such as Fe₃O₄ and CoFe₂O₄ grown on BaTiO₃, the strain is strongly reduced for films thicker than the coherent critical thickness through the onset of misfit dislocations;^{24,25} in the case of Fe₃O₄/BaTiO₃(100), the experimental evidence points to full relaxation at the temperature of growth.¹⁷ Here, we do not take explicitly into account the effect of dislocations to the magnetoelastic energy, but instead account for strain relaxation by adjusting the lattice parameter of the magnetic film so that the correct strain value is obtained at the measurement temperature, as will be discussed in more detail below. We consider three magnetic systems that have been studied experimentally and which are of particular interest: CoFe₂O₄,¹³ Fe₃O₄,^{16,17} and Fe films¹⁴ grown on BaTiO₃. In Table I, we list the relevant materials parameters for these magnetic systems.

A. Fe₃O₄/BaTiO₃(100) epitaxial films

We consider first the case of Fe₃O₄/BaTiO₃(100) epitaxial films, where experimentally it is found that the Fe₃O₄ has a residual strain at room temperature with a sign that is opposite that expected from the lattice mismatch with BaTiO₃; this has been explained as due to strain relaxation at the temperature of growth, followed by an in-plane dilation due to the abrupt increase in the cell parameters of BaTiO₃ at the cubic to tetragonal phase transition.¹⁷ Therefore, the magnetoelastic anisotropy contribution to the magnetic energy is very different from that expected for a fully strained Fe₃O₄ film: while the values for the magnetostriction coefficients of Fe₃O₄ favor a state of in-plane magnetization, experimentally a non-zero perpendicular remanence and magnetic anisotropy are observed.^{16,17} In Fig. 2 we present our estimate for the variation of the magnetoelastic anisotropy constants as a function of temperature, where we took into account the temperature variation of the lattice constants of BaTiO₃ and Fe₃O₄.^{31,32} The strain relaxation was taken into account, in a first approximation, by shifting the lattice constant of magnetite such that the out of plane strain at room temperature coincides with the experimental value of -0.62% for tetragonal domains.¹⁷ This assumes that the misfit dislocation density remains constant throughout the temperature range and across the phase transitions of BaTiO₃. One indication that this approach is a simplification over the real processes occurring in the magnetite film is the fact that, as observed in Fig. 2, the strain in the cubic phase does not drop to zero as the temperature approaches the growth temperature, indicating that a strong temperature dependence of the lattice constant, or misfit dislocation density, may occur in the high temperature range. The temperature variation of the magnetic anisotropies is instructive, however, and helps explain the variations in

TABLE I: Room temperature material parameters for Fe, Fe₃O₄ and CoFe₂O₄. The elastic constants c_{ij} are given in erg/cm³, the magnetization M_s in emu/cm³, and the cubic magnetocrystalline anisotropy K_1 in erg/cm³ (a is the lattice constant).

Material	a (Å)	$10^{-12}c_{11}$	$10^{-12}c_{12}$	$10^{-12}c_{44}$	$10^6\lambda_{100}$	$10^6\lambda_{111}$	M_s	$10^{-6}K_1$
Fe ^g	2.866	2.322	1.356	1.170	24.1	-22.7	1717	0.48
Fe ₃ O ₄ ^a	8.397	2.73	1.06	0.97	-19.5	77.6	471	-0.110
CoFe ₂ O ₄	8.381 ^b	2.57 ^c	1.500 ^c	0.853 ^c	-590 ^d	120 ^d	425 ^e	1.8 ^f

^aFrom Ref. 26.

^bFrom Ref. 27.

^cFrom Ref. 28.

^dFrom Ref. 29, for single crystalline Co_{0.8}Fe_{2.2}O₄.

^eFrom Ref. 29.

^fFrom Ref. 29, for sample with composition Co_{1.1}Fe_{1.9}O₄.

^gFrom Ref. 30.

the magnetic properties observed experimentally. Focusing on the out of plane anisotropy constant K_p first, we see that negative out of plane strains favor perpendicular anisotropy, which are large for the rectangular domains of the tetragonal phase and for the oblique domains of the orthorhombic and rhombohedral phases; they are smaller by a factor of about 2 for the square domains of the tetragonal phase and the rectangular domains of the orthorhombic phase. Depending on the particular domain path followed by the BaTiO₃ substrate, it is clear that large changes in the magnetic anisotropies may follow. For example, the experimental results of Vaz et al.¹⁷ can be explained if, starting from a rectangular domain at room temperature, the BaTiO₃ surface reverts to a rectangular domain in the orthorhombic phase, corresponding to a drop in the perpendicular magnetic anisotropy, followed by an increase in K_p in the rhombohedral phase. The in-plane anisotropies are also significant, but they tend to be smaller than the perpendicular anisotropies. The presence of multidomains in BaTiO₃ also tends to average out the in-plane effective anisotropy.

It must be emphasized that a negative K_p is not sufficient to yield perpendicularly magnetized films, since the in-plane magnetostatic (shape) anisotropy must also be overcome, and the latter is on the order of $2\pi M_s^2 = 1.39 \times 10^6$ erg/cm³ for magnetite, assuming bulk magnetization (thin magnetite films are known to exhibit a slightly reduced magnetization, which would lead to a smaller magnetostatic energy).^{33,34,35} This value would imply that the Fe₃O₄/BaTiO₃ films would remain in-plane magnetized, but this assumes a state of uniform strain; in real films, one may expect larger interface strains that could give rise to larger magnetoelastic anisotropies than those predicted in our simple model calculations.

B. CoFe₂O₄/BaTiO₃(100) epitaxial films

We consider here the case when the CoFe₂O₄ film is fully strained to the BaTiO₃ substrate, a situation which is expected to occur at thicknesses below the coherent growth thickness. Large changes in magnetization as

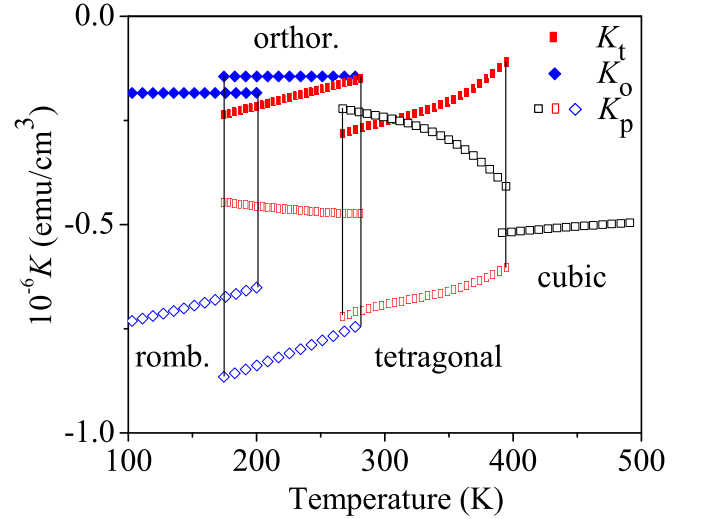


FIG. 2: Variation of the magnetoelastic anisotropy constants of partially strained Fe₃O₄/BaTiO₃(001). Square symbols correspond to anisotropy in planar square domains, diamonds to oblique domains, and rectangles to rectangular domains; full symbols are for in-plane anisotropies, empty symbols for the perpendicular anisotropy constants.

a function of temperature have been reported for partially relaxed 50-150 nm CoFe₂O₄/BaTiO₃(100) epitaxial films.¹³ Cobalt ferrite (CoFe₂O₄) is characterized by very large magnetostriction coefficients and has been a material of choice for strain-driven composite multiferroics.⁶ It is ferrimagnetic with a Curie temperature of 790 K and is predicted to be nearly fully spin polarized.^{36,37}

The calculated magnetoelastic anisotropies across the different phases of BaTiO₃ using the expressions derived above are shown in Fig. 3, where we took into account the temperature variation of the lattice parameter of CoFe₂O₄.^{38,39} The out of plane anisotropies for the fully strained film are very large, of the order of 9×10^7 erg/cm³, and favor in-plane magnetization, so we have omitted these from the figure. In the cubic phase, the biaxial strain contributes only to second order to the magnetic anisotropy,⁴⁰ and the in-plane magnetic anisotropy

will be dominated by the magnetocrystalline anisotropy, of the order of 2×10^6 erg/cm³ (favoring the in-plane $\langle 100 \rangle$ directions). In the tetragonal phase, the rectangular domains induce a very large uniaxial anisotropy favoring the direction of in-plane compression (x axis in Fig. 1). In the orthorhombic phase, the distortion induced by the rectangular domains is smaller, and the magnetic anisotropy decreases slightly. The oblique distortions of the orthorhombic and rhombohedral phases induce relatively small magnetic anisotropies due to the much smaller value of λ_{111} , and the magnetic anisotropy may be dominated by the magnetocrystalline anisotropy, assuming that a value comparable to the tabulated room temperature value still holds.

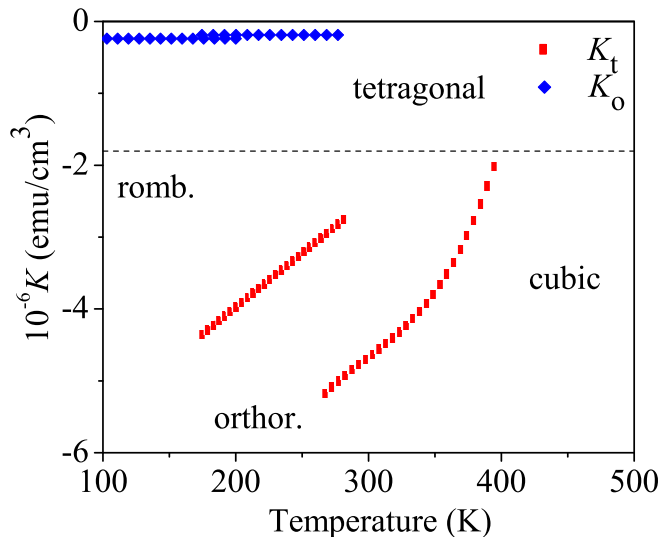


FIG. 3: Variation of the in-plane magnetoelastic anisotropy constants of fully strained $\text{CoFe}_2\text{O}_4/\text{BaTiO}_3(100)$. Diamonds correspond to anisotropy in oblique domains; rectangles to rectangular domains; the dashed line corresponds to the room temperature magnetocrystalline anisotropy of bulk $\text{Co}_{1.1}\text{Fe}_{1.9}\text{O}_4$ (which favors the $\langle 100 \rangle$ directions).

Magnetization versus temperature measurements of epitaxial $\text{CoFe}_2\text{O}_4/\text{BaTiO}_3(001)$ films have been presented by Chopdekar and Suzuki¹³ for a 56 nm film under an applied magnetic field $H = 50$ kOe, along the nominal $[100]$ and $[010]$ in-plane directions. Even at this very large magnetic field, large jumps in the magnetization are observed at the tetragonal to orthorhombic and orthorhombic to rhombohedral phase transitions of BaTiO_3 . As the temperature is lowered from 350 K to 150 K, the magnetization for $\mathbf{H} \parallel [010]$ direction increases slightly at 290 K, and then decreases more drastically at 190 K; when $\mathbf{H} \parallel [100]$ direction, the magnetization behaves in the opposite fashion, starting and ending at values that are close to those of the magnetization when the magnetic field is applied along the $[010]$ direction. These changes in the magnetization can be understood by assuming predominantly square domains in the tetragonal phase of BaTiO_3 , which give similar anisotropies for both the

$[100]$ and $[010]$ directions; the presence of a small number of rectangular domains, or a small imbalance in the two possible rectangular domains, would give rise to a small uniaxial magnetic anisotropy favoring, say, the $[010]$ direction; these domains would either remain rectangular in the orthorhombic phase or revert to oblique domains. In the orthorhombic phase, the square domains change to rectangular and the increase in magnetic energy along the $[100]$ direction (leading to a smaller magnetization) could result from rectangular domains that are predominantly elongated along the $[100]$ direction (the easy axis direction is along the direction of compression for CoFe_2O_4 , which has $b_1 > 0$). The transition to the rhombohedral phase would lead to similarly small magnetic anisotropies for both $[100]$ and $[010]$ directions, leading to an increase in magnetic energy for the $[010]$ direction, and a decrease along the $[100]$ direction. Despite clear hysteresis in the ferroelectric transitions of BaTiO_3 , the observation of reproducible paths in the magnetic behavior suggests that also the ferroelectric domains of BaTiO_3 also follow similar switching paths with thermal cycling.

C. $\text{Fe}/\text{BaTiO}_3(100)$ epitaxial films

As a final example, we consider the case of Fe, where the relatively small lattice mismatch with BaTiO_3 of -1.4% should allow the growth of fully strained epitaxial films. Further interest in this particular system stems from recent theoretical predictions of surface magneto-electric effects induced by spin-polarized screening at the Fe/BaTiO_3 interface.⁴¹ The calculated magnetoelastic anisotropies for the different phases of BaTiO_3 are shown in Fig. 4. Due to the strong crystal field of metallic Fe, the orbital moment is quenched, and the magnetic anisotropies are relatively small in this system. It can be seen that for $\text{Fe}/\text{BaTiO}_3(100)$, the perpendicular magnetoelastic anisotropies favor perpendicular magnetization, but given the very large magnetostatic energy of Fe ($2\pi M_s^2 = 1.85 \times 10^7$ erg/cm³), an in-plane magnetized state is energetically more favorable. The magnetoelastic in-plane anisotropies are also relatively small due to the small strains involved, but are likely to strongly influence the switching behavior of the Fe film.

Sahoo et al.¹⁴ have reported magnetic measurements on a 10 nm polycrystalline Fe film deposited on a $\text{BaTiO}_3(100)$ substrate at 373 K, where the magnetization under a small applied magnetic field (20-80 Oe) shows sudden jumps at the phase transitions of BaTiO_3 . Although the Fe film is likely to be fully relaxed, the relative changes in magnetic anisotropy can still be compared qualitatively with the results shown in Fig. 4. For the particular field direction, which is applied in the plane of the film, the magnetization is found to increase steeply with decreasing temperature at both ~ 278 K and ~ 183 K, indicating a decrease in the magnetic anisotropy along this direction. The results shown in Fig. 4 suggest that the magnetic field is being applied along the a direc-

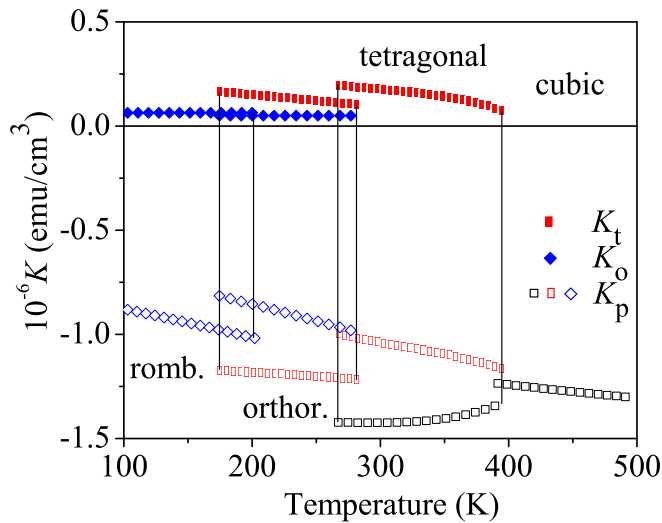


FIG. 4: Variation of the magnetoelastic anisotropy constants of fully strained Fe/BaTiO₃(100). Square symbols correspond to anisotropy in planar square domains, diamonds to oblique domains, and rectangles to rectangular domains. Filled symbols are for in-plane anisotropies and empty symbols are for the perpendicular anisotropy constants.

tion of the rectangular domains of the tetragonal phase, which corresponds to a hard axis direction (in Fe this is the direction of compression, since $b_1 < 0$) and that the dominant planar domains in the orthorhombic phase of BaTiO₃ are rectangular, compressed in this direction. This also agrees with the measured temperature variation of the perpendicular magnetization, where an increase at ~ 278 K is followed by a decrease at ~ 183 K with decreasing temperature, in agreement with the variation found

for K_p , shown in Fig. 4.

IV. CONCLUSIONS

Explicit expressions for the magnetoelastic anisotropy constants have been derived for arbitrary in-plane distortions of the unit cell of cubic systems and applied to the particular case where those distortions are induced by elastic coupling to BaTiO₃ substrates. BaTiO₃ undergoes a series of phase transitions as a function of temperature and has been employed to study the effect of strain on the magnetic properties of epitaxial magnetic films and, in particular, aimed at designing new magnetoelectric composite systems. Since the elastic properties of ferroelectrics, and BaTiO₃ in particular, can be modulated by electric fields via the piezoelectric effect, modulation of magnetism via electric fields is possible. We have considered three particular magnetic systems that have been studied experimentally (Fe₃O₄, CoFe₂O₄, and Fe), and explained the observed magnetic behavior in terms of the changes in magnetic anisotropies arising from strain induced in the different phases of BaTiO₃. This work provides a quantitative account of the experimental observations and opens the way to a more calibrated targeting of the properties of heterosystems for optimum magnetoelectric coupling effects.

Acknowledgments

This work was supported by the NSF through MRSEC DMR 0520495 (CRISP).

- ¹ S. M. Skinner, IEEE Trans. Parts Mater. Pack. **PMP-6**, 68 (1970).
- ² G. A. Smolenskii and I. E. Chupis, Sov. Phys. Usp. **25**, 475 (1982).
- ³ H. Schmid, Ferroelectrics **162**, 317 (1994).
- ⁴ M. Fiebig, J. Phys. D: Appl. Phys. **38**, R123 (2005).
- ⁵ K. Mori and M. Wuttig, Appl. Phys. Lett. **81**, 100 (2002).
- ⁶ H. Zheng, J. Wang, S. E. Lofland, Z. Ma, L. Mohaddes-Ardabili, T. Zhao, L. Salamanca-Riba, S. R. Shinde, S. B. Ogale, F. Bai, et al., Science **303**, 661 (2004).
- ⁷ F. Zavaliche, H. Zheng, L. Mohaddes-Ardabili, S. Y. Yang, Q. Zhan, P. Shafer, E. Reilly, R. Chopdekar, Y. Jia, P. Wright, et al., Nano Lett. **5**, 1793 (2005).
- ⁸ C. Thiele, K. Dörr, O. Bilani, J. Rödel, and L. Schultz, Phys. Rev. B **75**, 054408 (2007).
- ⁹ H. J. A. Molegraaf, J. Hoffman, C. A. F. Vaz, S. Gariglio, D. van der Marel, C. H. Ahn, and J.-M. Triscone (2008), unpublished.
- ¹⁰ D. Dale, A. Fleet, J. D. Brook, and Y. Suzuki, Appl. Phys. Lett. **82**, 3725 (2003).
- ¹¹ M. K. Lee, T. K. Nath, C. B. Eom, M. C. Smoak, and F. Tsui, Appl. Phys. Lett. **77**, 3547 (2000).
- ¹² W. Eerenstein, M. Wiora, J. L. Prieto, J. F. Scott, and N. D. Mathur, Nature Mater. **6**, 348 (2007).
- ¹³ R. V. Chopdekar and Y. Suzuki, Appl. Phys. Lett. **89**, 182506 (2006).
- ¹⁴ S. Sahoo, S. Polisetty, C.-G. Duan, S. S. Jaswal, E. Y. Tsybal, and C. Binek, Phys. Rev. B **76**, 092108 (2007).
- ¹⁵ M. Ziese, A. Bollero, I. Panagiotopoulos, and N. Moutis, Appl. Phys. Lett. **88**, 212502 (2006).
- ¹⁶ H. F. Tian, T. L. Qu, L. B. Luo, J. J. Yang, S. M. Guo, H. Y. Zhang, Y. G. Zhao, and J. Q. Li, Appl. Phys. Lett. **92**, 063507 (2008).
- ¹⁷ C. A. F. Vaz, J. Hoffman, A.-B. S. Posadas, and C. H. Ahn (2008), unpublished.
- ¹⁸ F. Jona and G. Shirane, *Ferroelectric crystals* (Pergamon Press, New York, 1962).
- ¹⁹ M. Adachi, Y. Akishige, T. Asahi, K. Deguchi, K. Gesi, K. Hasebe, T. Hikita, T. Ikeda, M. K. Y. Iwata, T. Mitsui, et al., in *Landolt-Börnstein - Group III: Crystal and Solid State Physics*, edited by Y. Shiozaki, E. Nakamura, and T. Mitsui (Springer-Verlag, Berlin, 2002), vol. 36A1, p. 67.
- ²⁰ S. Chikazumi, *Physics of Ferromagnetism* (Clarendon Press, Oxford, 1997), 2nd ed.

- ²¹ A. E. H. Love, *A treatise on the mathematical theory of elasticity* (Cambridge University Press, Cambridge, 1920), 3rd ed.
- ²² W. J. Carr, Jr., in *Encyclopedia of Physics*, edited by S. Flügge (Springer Verlag, Berlin, 1966), vol. XVIII/2, p. 274.
- ²³ C. A. F. Vaz, J. A. C. Bland, and G. Lauhoff, Rep. Prog. Phys. **71**, 056501 (2008).
- ²⁴ J. W. Matthews, in *Epitaxial Growth*, edited by J. W. Matthews (Academic Press, Inc., 1975), vol. B, p. 559.
- ²⁵ D. Hull and D. J. Bacon, *Introduction to dislocations* (Pergamon Press, 1984), 3rd ed.
- ²⁶ R. A. Lefever, in *Landolt-Börnstein - Group III: Crystal and Solid State Physics*, edited by K.-H. Hellwege and A. M. Hellwege (Springer-Verlag, Berlin, 1970), vol. 4b, p. 65.
- ²⁷ H. V. Philipsborn and L. Treitinger, in *Landolt-Börnstein - Group III: Crystal and Solid State Physics*, edited by K.-H. H. und A. M. Hellwege (Springer-Verlag, Berlin, 1980), vol. 12b, p. 54.
- ²⁸ Z. Li, E. S. Fisher, J. Z. Liu, and M. V. Nevitt, J. Mater. Sci. **26**, 2621 (1991).
- ²⁹ V. Folen, in *Landolt-Börnstein - Group III: Crystal and Solid State Physics*, edited by K.-H. H. und A. M. Hellwege (Springer-Verlag, Berlin, 1970), vol. 4b, p. 366.
- ³⁰ M. B. Stearns, in *Landolt-Börnstein - Group III: Crystal and Solid State Physics*, edited by H. P. J. Wijn (Springer-Verlag, Berlin, 1986), vol. 19a, p. 24.
- ³¹ L. A. Shebanov, Phys. Stat. Sol. (a) **65**, 321 (1981).
- ³² J. Yoshida and S. Iida, J. Phys. Soc. Japan. **47**, 1627 (1979).
- ³³ D. T. Margulies, F. T. Parker, F. E. Spada, R. S. Goldman, J. Li, R. Sinclair, and A. E. Berkowitz, Phys. Rev. B **53**, 9175 (1996).
- ³⁴ D. T. Margulies, F. T. Parker, M. L. Rudee, F. E. Spada, J. N. Chapman, P. R. Aitchison, and A. E. Berkowitz, Phys. Rev. Lett. **79**, 5162 (1997).
- ³⁵ J.-B. Moussy, S. Gota, A. Bataille, M.-J. Guittet, M. Gautier-Soyer, F. Delille, B. Dieny, F. Ott, T. D. Doan, P. Warin, et al., Phys. Rev. B **70**, 174448 (2004).
- ³⁶ M. Pénicaud, B. Siberchicot, C. B. Sommers, and J. Kübler, J. Magn. Mater. **103**, 212 (1992).
- ³⁷ V. N. Antonov, B. N. Harmon, and A. N. Yaresko, Phys. Rev. B **67**, 024417 (2003).
- ³⁸ Y. Iwasaki, M. Kaneko, K. Hayashi, Y. Ochiai, M. Hayakawa, and K. Aso, J. Phys. E: Sci. Instrum. **22**, 498 (1989).
- ³⁹ D. Taylor, British Ceramic, Transactions and Journal **84**, 121 (1985).
- ⁴⁰ C. A. F. Vaz and J. A. C. Bland, J. Appl. Phys. **89**, 7374 (2001).
- ⁴¹ C.-G. Duan, S. S. Jaswal, and E. Tsymbal, Phys. Rev. Lett. **97**, 047201 (2006).